# EFFECT OF WO$_3$ DOPING CONCENTRATION ON THE PROPERTIES V$_2$O$_5$ THIN FILMS PREPARED BY VACUUM DEPOSITION TECHNIQUE

P. Yuvaraj[1], A. Priya[1], S. Pavithra[1], J. Jayachitra[2], N. Sivakumar[1*]

[1]PG and Research Department of Physics, Chikkaiah Naicker College, Erode, Tamilnadu 638004, India.
[2]Department of Physics, L.R.G government Arts College for Women, Tirupur, Tamilnadu 641604, India.

*Abstract: Vanadium pentoxide (V$_2$O$_5$) is the promising material for energy storage applications. In the present work pure and WO$_3$ doped (2, 4, 6 and 8 wt. %) V$_2$O$_5$ thin films were prepare by vacuum deposition technique on ITO substrate. The structural behavior has been carried out by XRD and crystalline WO$_3$ doped vanadium pentoxide (V$_2$O$_5$) exhibits orthorombic structure. The surface morphological images of the WO$_3$ doped V$_2$O$_5$ thin films shows granular surface which has been investigated by FESEM. Optical behavior indicates that the band gap decreasing (from 2.98 to 2.77 ev) with increasing doping concentration. Raman spectra were studied, in which several bands observed for these thin films have been explained on the basis of different bending, stretching band lattice phonon vibration modes occurring in the films. The electrochemical analysis results shows the WO$_3$ doped V$_2$O$_5$ exhibits the capacity of about 260 mAh/g after 100 cycles.*

*Keywords - vacuum deposition technique; vanadium pentoxide; structural, Optical and electrochemical properties*

## I. INTRODUCTION

Transition metal oxides are conventional special interest due to their higher stability as compared to organic electrochromism. In recent decades, vanadium oxides have been obtained a lot of attention, because of the enhancement of structural, optical, electronic and electrochemical properties which compared to other oxide materials. This type of vanandium oxides are suitable for different applications such as sensors [1], catalysis [2], capacitors [3], lithium ion batteries [4] and electrochromic devices [5]. In general, vanadium pentoxide (V$_2$O$_5$) is a non-stoichiometric material, which is known for its catalytic properties in oxidation reactions. It has been characterized by a semiconductor – to – metal transition occurring from a reversible change in the crystalline structure as a function of the temperature [6, 7]. Moreover, V$_2$O$_5$ is the most widely studied as a cathodic material presenting high capacity upon the reversible intercalation/deintercalation of Li$^+$ due to its layered structure [8] and its high valence state [9]. Day and Sullivan [10] were studied and filed the first report related to the V$_2$O$_5$ can be used as a cathode material. The optical properties of vanadium dioxide are analyzed by a sharp decrease in optical transmission in the infrared spectrum during the semiconductor – metal transition. Due to this inconsistent behavior, vanadium dioxide has been presented as an attractive thin film material for electrical and optical switches and solar energy control for windows. Vanadium can be adopt a single valance in oxidation states from V$^{2+}$ to V$^{5+}$ in the form of VO [11], V$_2$O$_3$[12], VO$_2$[13], and V$_2$O$_5$[14]. The nanostructured of V$_2$O$_5$ is characterized by a large electrochemical surface area and good inter-connectivity for electric conductivity. Though, the lithiation processes in V$_2$O$_5$ bulk are relatively slow due to the low electric conductivity ($10^{-3}$ to $10^{-2}$ S.m$^{-1}$) and low Li$^+$ diffusion coefficients ($10^{-3}$ to $10^{-12}$ cm$^2$.s$^{-1}$) [15,16].

In order to improve the electric conductivity and electrochromic properties, the binary combinations of oxides have been investigated. Promising effects on the host electrochromic materials are increased the efficiency, improved stability, a larger switching potential range or faster reaction kinetics. Granqvist [17] has reviewed the mixed metal oxides and reported valuable summary. In previous investigations on V$_2$O$_5$ added with metal oxide (MO$_3$) have showed the enhancement over the basic electrochromic properties of V$_2$O$_5$. Among those transition metal oxides, tungsten trioxide (WO$_3$) has wide band gap in the range of E$_g$ = 2.5 – 2.8 eV at room temperature and appears to be the best electrochromic compound [18]. Tungsten has shown the most effective dopant ion in reducing the metal-semiconductor transition of vanadium oxide with lower Tc of 25 ℃ which as reported by Blackman et al [19]. Also, vanadium and tungsten oxides are important due to their current and substantial technological applications, in which tungsten has the similar ionic radius with V$_2$O$_5$ in the highest oxidation state [20].

Composite WO$_3$ added with MO$_x$ films have been prepared by different methods such as sol-gel deposition [21], sputtering [22], electron-beam evaporation [23], and vaccum evaporation [24], etc. Moreover, Li et al [25] have reported W doped V$_2$O$_5$ nanotubes which have been prepared by self-assembling process. The novel tungsten-doped vanadium oxide xerogel films were prepared by the sol-gel and hydrothermal route for electrochromic electrodes [26].

In our present work, we have selected a vacuum deposition technique for preparing pure and WO$_3$ doped V$_2$O$_5$ thin films on ITO substrate. The effect of WO$_3$ doped V$_2$O$_5$ with different weight percentage (2, 4, 6 and 8 wt. %) has been systematically studied. Furthermore, the structural, surface morphological, optical and electrochemical properties of pure and WO$_3$ doped V$_2$O$_5$ thin films were investigated.

## II. EXPERIMENTAL DETAILS

$V_2O_5$ and $WO_3$ powders (99.999% - sigma aldrich) were taken in different weight percentage (2, 4, 6 and 8 wt. %) and grinded for 3 hours with the help of mortar and sintered at 400 $^0$C for 5 hour. The dimensions of substrates were 1.5 cm x 9 cm x 0.1 cm and these substrates were cleaned before deposition with acetone followed by isopropyl alcohol and rinsed in deionized water. The thermal evaporation technique (HHV 12" Vacuum coating unit Model 12A4D) was used to deposit pure $V_2O_5$ and $WO_3$ doped $V_2O_5$ thin films of thickness 100 nm on ITO coated glass substrates at 300 $^o$C temperature under high vacuum (5.5x $10^{-5}$ Torr).The distance between source and substrate was about 180 mm and a tantalum boat was used inside the vacuum chamber. The thickness of the films and evaporation/deposition rate were examined by quartz crystal monitor which was placed just below the substrate holder.

## III. RESULTS AND DISCUSSION

*A. XRD analysis*

      The structural properties of pure $V_2O_5$ and $WO_3$ doped $V_2O_5$ thin films were investigated by XRD measurements. Figure 1 shows, the XRD patterns which are indexed to orthorhombic $V_2O_5$ phase (JCPDS 41-1426) having lattice parameters a = 11.516 Å, b = 3.56 Å and c= 4.37 Å. The diffraction peak at 20.275° is indicating the crystalline of $V_2O_5$ phase with the space group C2/c. The d-spacing values of all diffraction peaks are identical to those of the orthorhombic crystalline phase $V_2O_5$ (Space Group: *Pmmn*). Previous reports are available for $V_2O_5$ with the same phase [27].

As the doping concentration increases, the intensity of the preferred orientation of (0 0 1) indicates that the decreased crystallinity. In the present XRD result, (0 0 1) plane has the highest intensity for pure $V_2O_5$ which is similar to previous literature report [28]. Ashvani kumar et al [29] have observed that the high substrate temperature leads to higher oxygen vacancy in the $V_2O_5$ phase causing shift to lower valence state. The induced vacancy can go ahead to partial collapse of the V-O layer assisting the formation of $V_2O_5$ phase [30-31].
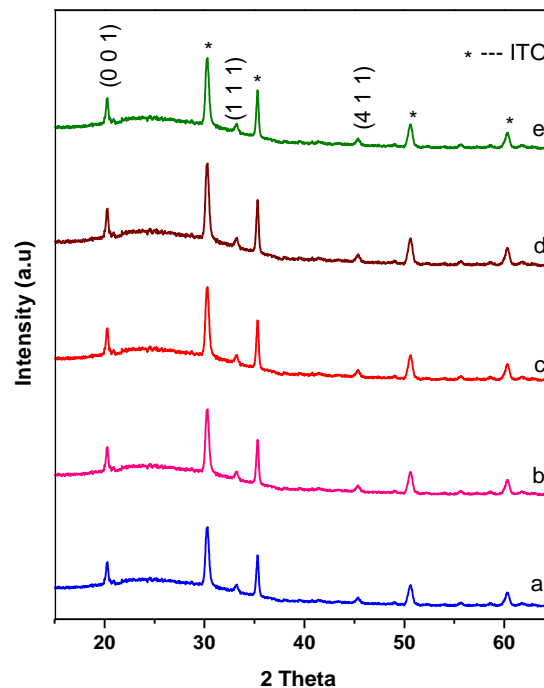


Fig.1. XRD patterns of pure $V_2O_5$ and $WO_3$ doped $V_2O_5$ thin films
(a) pure (b) 2 at % $WO_3$ (c) 4 at % $WO_3$ (d) 6 at % $WO_3$ (e) 8 at % $WO_3$

The increasing of $WO_3$ concentrations shows that the peaks are shifted (between the diffraction angles (2θ) of 20.275° and 20.484°). As the doping concentrations of $WO_3$ increase, no other peak is observed for $WO_3$ in the $WO_3$ doped $V_2O_5$ films using Vacuum deposition technique. The reasons are (i) the minimum amount of $WO_3$ concentration may present in the form of very small clusters in $V_2O_5$ lattices, therefore, it might be very complex to detect by XRD instrument and (ii) probably placed in the grain boundaries of the $V_2O_5$ nanocrystals - or distributed atomically within the $V_2O_5$ lattice (e.g. by occupying the central positions of the tetrahedral arrangement or by replacing some V atoms in their lattice position) [32-34].

TABLE.1. THE MICROSTRUCTURAL PROPERTIES OF THE PURE $V_2O_5$ AND $WO_3$ DOPED $V_2O_5$ THIN FILMS

| Materials | Diffraction angle 2θ (deg) | Plane | Crystallite size (D) (nm) | Micro strain (ε) (x $10^{-3}$ lines$^{-2}$ m$^{-4}$) | Dislocation density (x$10^{14}$cm$^{-2}$) | Stacking Fault (x $10^{-2}$) | Texture Coefficient (Tc) |
|---|---|---|---|---|---|---|---|
| $V_2O_5$ | 20.275 | 0 0 1 | 42 | 0.822 | 0.193 | 5.589 | 1.01 |
| 2% $WO_3$ | 20.381 | 0 0 1 | 37 | 0.943 | 0.419 | 7.265 | 0.89 |
| 4% $WO_3$ | 20.484 | 0 0 1 | 34 | 1.102 | 0.301 | 8.450 | 0.87 |
| 6% $WO_3$ | 20.478 | 0 0 1 | 28 | 1.234 | 0.693 | 12.140 | 0.92 |
| 8% $WO_3$ | 20.372 | 0 0 1 | 24 | 1.407 | 0.806 | 16.935 | 1.06 |

Table 1 shows the microstructural properties of pure $V_2O_5$ and $WO_3$ doped $V_2O_5$ thin films for the preferred orientation of (0 0 1) plane. The crystallite size (D) [35], microstrain (ε), dislocation density (δ), stacking fault (SF) and texture coefficient ($T_c$) values can be obtained [36].

The crystallite size (D) of the preferred orientation (0 0 1) plane is decreased from 42 to 24 nm for increasing the doping concentration of $WO_3$ from 0 to 8 wt. % as shown in Table 1. Microstrain, dislocation density and stacking fault have increased with increasing of doping concentration (Table 1). Madhavi et al. [37] observed that decreasing of crystallite size and increasing of strain by increasing of $WO_3$ doping concentration on $V_2O_5$. Lethy et al. [38] also reported that the microstructural investigation shows that incorporation of titanium stronglydisturbs the $WO_3$ lattice and decreases the crystallite size.

*B. Field Emission Surface Morphology studies*
The surface structure and grain arrangement were analyzed by the FESEM results. Surface images of the pure $V_2O_5$ and $WO_3$ doped (4 and 8 wt. %) $V_2O_5$ samples are shown in figure 2. The image of pure $V_2O_5$ sample (Fig. 2a) shows that the surface appears to be spherical in shape with spongy bush like structure, also with different grain size and free of grain boundaries. Previous reports [39, 40] shown the similar morphology for $V_2O_5$ film sample deposited at 400 °C. By increasing $WO_3$ doped (4 and 8 wt. %) in $V_2O_5$ samples (Fig. 2b and 2c), shown that the shape of the grains change into the mixed cubical and monoclinic phases. From the FESEM images, the average particle size has been observed to be in the range of ~ 25 nm for pure $V_2O_5$ samples and for $WO_3$ doped (4 and 8 wt. %) samples ~21 nm and ~18 nm respectively. Therefore, it is evident that, from these FESEM images, the addition of $WO_3$ in $V_2O_5$ resulted in decrease in the average particle size
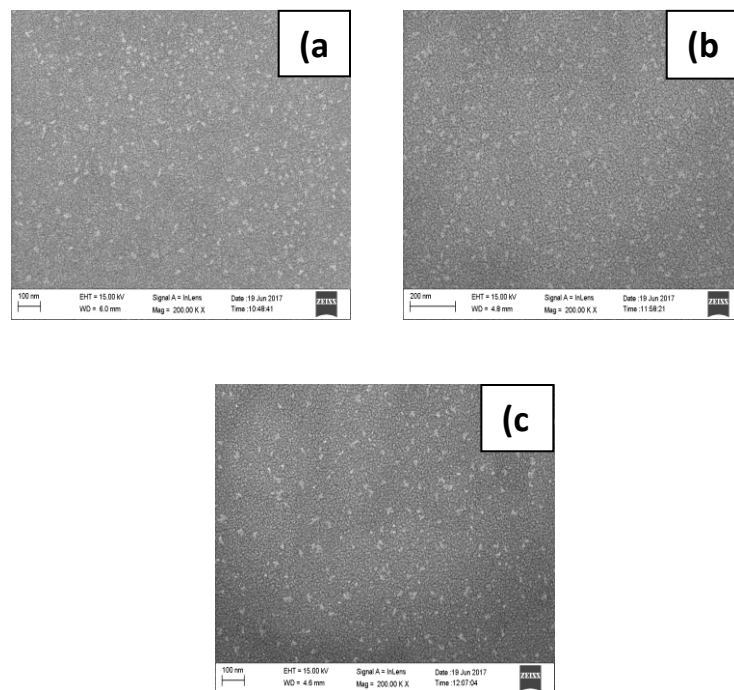


Fig.2. FESEM images of pure $V_2O_5$ and $WO_3$ doped $V_2O_5$ thin films,
(a)       pure (b) 4 at % $WO_3$ (c) 8 at % $WO_3$
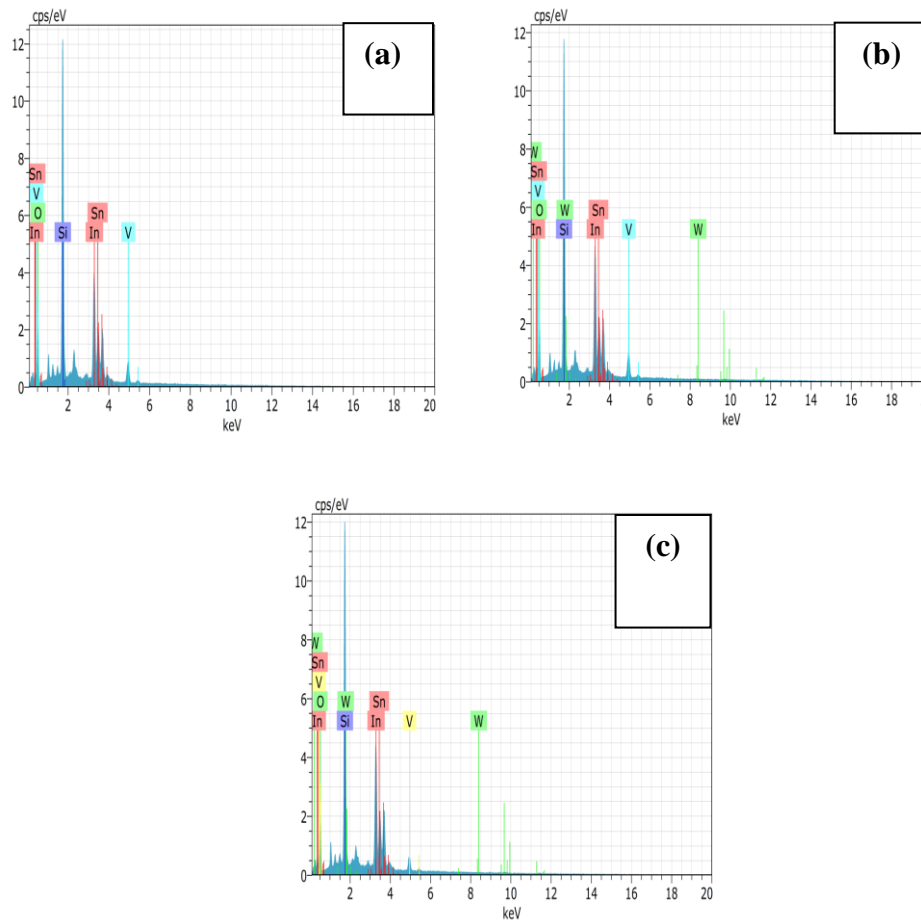
*C. Elemental Analysis*



Fig.3 EDAX images of pure $V_2O_5$ and $WO_3$ doped $V_2O_5$ thin films
(a) pure (b) 4 at % $WO_3$ (c) 8 at % $WO_3$

The stoichiometric ratio of the pure $V_2O_5$ and $WO_3$ doped $V_2O_5$ thin films were confirmed by the EDX spectra. The EDX spectra for $WO_3$ doped $V_2O_5$ thin films for different $WO_3$ doping concentration of 4 and 8 wt. % are shown in figure 3 (a-c). The EDX spectra reveal that the elements of W, V and O present in the prepared samples. As the doping concentration of W increases, the atomic percentage of W increases and O decreases in the present study. Table 2 represents that the atomic percentage of W and V increase and O decreases as increasing the doping concentration of W.

TABLE. 2 ATOMIC RATIO OF THE PURE $V_2O_5$ AND $WO_3$ DOPED $V_2O_5$ THIN FILMS

| WO$_3$ doping concentration (wt. %) | Atomic ratio (%) | | |
|---|---|---|---|
| | **W** | **V** | **O** |
| 0 | - | 30.67 | 69.33 |
| 4 | 2.13 | 30.83 | 67.04 |
| 8 | 3.95 | 29.93 | 66.12 |

*D. Optical Properties*

Figure 4 shows the optical absorption spectra of the pure $V_2O_5$ and $WO_3$ doped (2, 4, 6 and 8 wt. %) in the wavelength range of 300 to 900 nm. From the spectra, it has been clearly observed that the absorption edge shifted towards higher wavelengths with an increase in doped of $WO_3$. The shift in absorption of the doped sample might be due to change in electronic structure and surface morphology (grain boundaries and roughness) of films. The essential absorption of $V_2O_5$ is due to the electronic transitions from occupied 2p bands of oxygen to unoccupied 3d bands of vanadium ($O_{2p} \rightarrow V_{3d}$) [41]. Figure 4 shows the absorption spectra of the pure and $WO_3$ doped $V_2O_5$ nanoparticles with the absorption peaks at 416, 425, 436, 443 and 448 nm respectively. The band gap energy of pure and $WO_3$ doped $V_2O_5$ thin

films has been calculated by using the relation Eg = hc/$\lambda$ and the calculated values 2.98, 2.92, 2.84, 2.80 and 2.77 ev are correspond to pure, 2, 4, 6 and 8 wt. % $WO_3$ doped $V_2O_5$ thin films respectively. The observed Eg value is in good agreement with the Eg value determined in literature [42]. From these values it is concluded that the band gap energy decreases with $WO_3$ doping, which shows a red shift in wavelength.
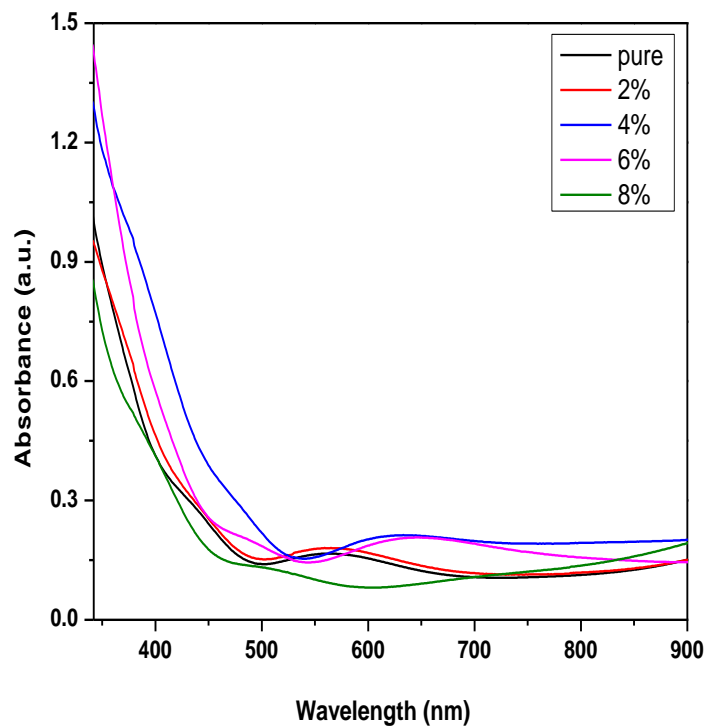


Fig.4. The Variation of % of Absorbance with Wavelength
(a)        pure (b) 2 at % $WO_3$ (c) 4 at % $WO_3$ (d) 6 at % $WO_3$ (e) 8 at % $WO_3$

*e. Raman Studies*

In order to study the phase and local structure of metal oxide thin films, Raman studies were carried out for pure $V_2O_5$ and doped $WO_3$ samples. The change in the molecular polarizability associated with the vibrational mode of the molecule gives rise to the Raman shift and presents valuable information about the structural units and different vibrational modes. Figure 5 shows the Raman spectra of pure $V_2O_5$ and doped $WO_3$ thin films. The orthorhombic structure of $V_2O_5$ compound belongs to space group of *Pmmn* ( $D_{2h}^{13}$ ) with Z=2 [43]. Also, it consists of chains of edge sharing $VO_5$ square pyramids, and V, $O_1$ and $O_2$ atoms occupy *4f Wyckoff* positions with site symmetry $C_s$. The 'V' atoms form five bonds with 'O' atoms. Normally the low frequency band in Raman spectra is attributed to lattice vibration of $V_2O_5$ [44]. Thus, the vibrational modes observed in the low frequency region are called external modes and the modes observed in the high frequency region are called internal modes. The internal modes include V-O stretching vibrations in the 500-1000 $cm^{-1}$ region and V-O-V bending vibrations in the range 200-500 $cm^{-1}$. The external vibrations, containing translation ($T_s$, $T_y$, $T_z$) and libration ($R_x$, $R_y$, $R_z$) modes viewed as relative motions of the structural units, lie in the low-frequency region.
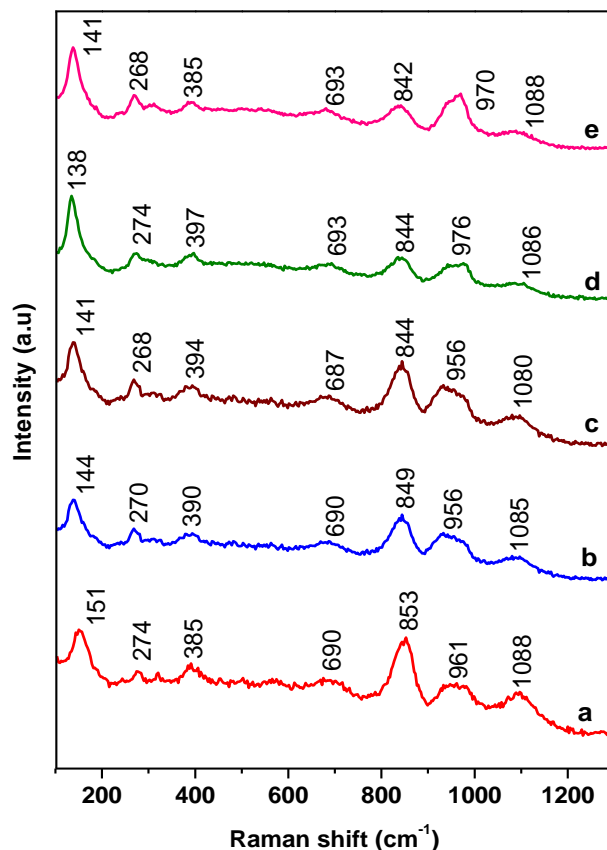
Fig. 5 Raman spectra of pure $V_2O_5$ and $WO_3$ doped $V_2O_5$ thin films
(a) Pure (b) 2 at % $WO_3$ (c) 4 at % $WO_3$ (d) 6 at % $WO_3$ (e) 8 at % $WO_3$

In our present studies, a band at 1088 cm$^{-1}$ has been assigned to stretching vibration mode of V-O$_1$ bond along O axis. The narrow peaks 961 cm$^{-1}$ are attributed to the stretching mode related to the $A_g$ symmetric vibrations of the shortest vanadium-oxygen bond (vanadyl V=O). The new peak observed at 853 cm$^{-1}$ is because of oxygen deficiency [45]. The band showing at 690 cm$^{-1}$ has been assigned to (V$_2$-O) stretching mode which results from corner shared oxygen common to two pyramids. Each $V_2O_5$ layer is built up from VO$_5$ square pyramids sharing edges and corners. The absence of two major bands at 520 cm$^{-1}$ and 650 cm$^{-1}$ confirms that V$_4$O bonds are not formed in this oxide film which as reported earlier [46]. The lattice vibration mode has appears very powerful at 151 cm$^{-1}$ which indicates organization of long range order in mixed oxide film. The shifting of 1088 cm$^{-1}$ band to 1080 cm$^{-1}$ for the doped $WO_3$ in $V_2O_5$ (Fig. 5 c) which indicates lengthening of O-V-O bond.

*F. Electrochemical Analysis*

The electrochemical performance has been analyzed through cyclic voltametry and the CV curve of pure and $WO_3$ doped $V_2O_5$ on ITO substrate are shown in figure 6. The electrochemical analysis was carried out in an three electrode cell in which the coated substrate was taken as an working electrode, AgCl as an reference electrode and platinum was taken as counter electrode. The theoretical specific capacity of $V_2O_5$ is about 273 mAh/g. After 100 cycles the pure $V_2O_5$ gives about 250 mAh/g with 80% of the capacity retention has been take place. But in $WO_3$ doped $V_2O_5$ has 90% of the capacity retention from its original value. It has been observed that the doping of $WO_3$ has increased the conductivity of the material causes easier movement ions during charging/discharging of the material which increases the cycling capacity and stability was also increased on doping of $WO_3$.
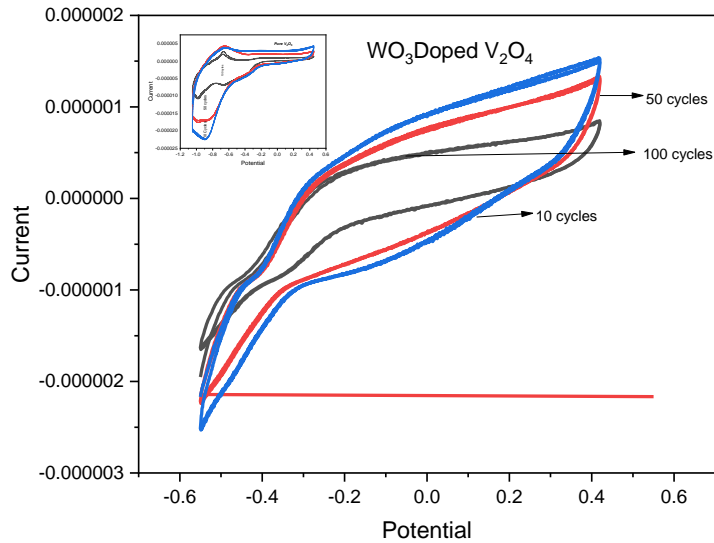
Fig.6. Potential and specific capacity of pure $V_2O_5$ and $WO_3$ doped $V_2O_5$ thin films
(a) pure (b) 2 at % $WO_3$ (c) 4 at % $WO_3$ (d) 6 at % $WO_3$ (e) 8 at % $WO_3$
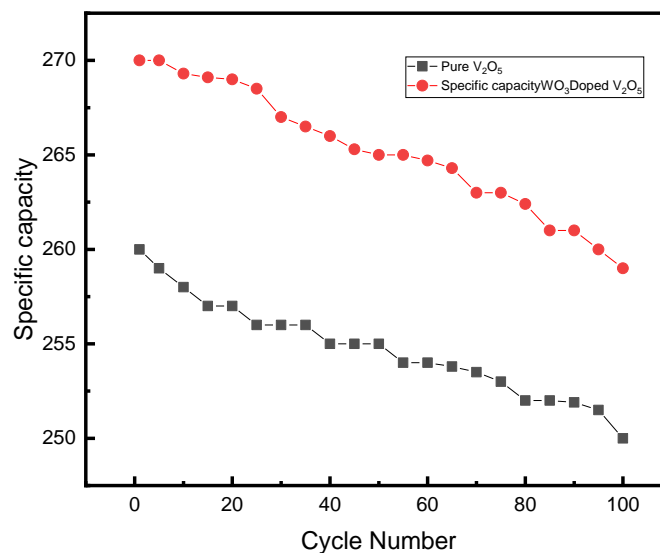


Fig.7. Specific capacity for varied cycle numbers for pure $V_2O_5$ and $WO_3$ doped $V_2O_5$ thin films
(a) pure (b) 2 at % $WO_3$ (c) 4 at % $WO_3$ (d) 6 at % $WO_3$ (e) 8 at % $WO_3$

## IV. CONCLUSION

Pure and $WO_3$ doped (2, 4, 6 and 8 wt. %) $V_2O_5$ thin films were prepared by the vacuum deposition technique on ITO substrate. The effect of $WO_3$ doping on the structural, morphological, compositional, optical and electrochromic properties of $V_2O_5$ thin films had been studied. It was observed that, Crystalline $WO_3$ doped vanadium pentoxide ($V_2O_5$) thin films with orthorhombic structure are found to have diffraction peaks correspond to (0 0 1), (1 1 1) and (4 1 1) crystal planes. The surface morphology has been carried out using FE-SEM, and from the image, the particle size was decreases on doping $WO_3$. The elemental confirmation has been done by using EDAX for both pure and $WO_3$ doped $V_2O_5$. From the UV result, the optical bandgap values of the films were in the range of 2.98 to 2.77 eV. The Raman studies indicates that, the shifting of 1088 cm$^{-1}$ band to 1080 cm$^{-1}$ for the doped $WO_3$ in $V_2O_5$ which represent the lengthening of O-V-O bond. Finally the electrochemical analysis results shows the $WO_3$ doped $V_2O_5$ gives the capacity of about 260 mAh/g after 100 cycles.

REFERENCES

[1] S. Zhuiykov, W. Wlodarski, Y.Li, Sensors Actuators B, 77 (2001) 484.

[2] D. Vernardou, E. Spanakis, G. Kenanakis, E. Koudoumas, N. Katsarakis, Mater. Chem. Phys., 124 (2010) 319.

[3] G. Wee, H.Z. Soh, Y.L.Cheah, S.G. Mhaisalkar, M. Srinivasan, J. Mater.Chem., 20 (2010) 6720.

[4] Y. Wang, G. Cao, Chem. Mater., 18 (2006) 2787.

[5] A. Talledo, C.G. Granqvist, Appl. Phys. A., 60 (1995) 521.

[6] R. Binions, G. Hyett, C. Piccirillo, I.P. Parkin, Journal of Materials Chemistry, 17 (2007) 4652.

[7] J.B.K. Kana, J.M. Ndjaka, B.D. Ngom, A.Y. Fasasi, O. Nemraoui, R. Nemutudi, D. Knoesen, M. Maaza, Optical Materials, 32 (2010) 739.

[8] O. Pelletier, P. Davidson, C. Bourgaux, C. Coulon, S. Regnault, J. Livage, Langmuir, 16 (2000) 5295.

[9] J. Wu, N. Membreno, W.-Y. Yu, J.D. Wiggins-Camacho, D.W. Flaherty, C.Buddie Mullins, K.J. Stevenson, J. Phys.Chem. C, 116 (2012) 21208.

[10] A.N. Day, B.P.Sullivan, Method of Preparing Cathodic Electrodes, U.S. Patent 3,655,585, 1972.

[11] M. Frandsen, J.Am.Chem.Soc. 74 (1952) 5046.

[12] B.S. Allimi, S.P. Alpay, T. Huang, J.I. Budnick, D.M. Pease, A.I. Frenkel, J.Mater.Res., 22 (2007) 2825.

[13] D. Verbardou, M.E. Pemble, D.W. Sheel, Chem. Vapor Depos,, 12 (2006) 263.

[14] D.Vernardou, P.Paterakis, H.Drosos, E.Spanakis, I.I. Povey, M.E.Pemble, E.Koudoumas, N. Katsarakis, Sol.Energy Mater. Sol. Cells, 95 (2011) 2842.

[15] Z. Tong, X. Zhang, H. Lv, N. Li, H. Qu, J. Zhao, Y. Li, X.Y. Liu, Adv.Mater.Interfaces, 2 (2015)1500230.

[16] Z. Tong, J. Hao, K. Zhang, J. Zhao, B.-L.Suc, Y. Li, J. Mater.Chem.C, 2 (2014) 3651.

[17] C. G. Granqvist, Handbook of Inorganic Electrochromic Materials, Elsevier, Amsterdam, 1995.

[18] C. G. Granqvist, Handbook of Inorganic Electrochromic Materials (Amsterdam: Elsevier Science) 1995.

[19] C. S. Blackman, C. Piccirillo, R. Binions, I.P. Parkin, Thin Solid Films, 517 (2009) 4565.

[20] B. A. Gee, A. Wong, J.Phy.Chem.B, 107 (2003) 8382.

[21] N. Ozer, C.M. Lampert, Thin Solid Films, 349 (1999) 205.

[22] G. Jia Fang, K.Yao, Z. Liu, Thin Solid Films, 394 (2002) 64.

[23] G.J. Fang, Z.L. Liu, Y.Q. Wang, H.H. Liu and K.L.Yao, J.Phys.D: Apply.Phy.. 33 (2000) 3018.

[24] K.C. Cheng, F.R. Chen, J.J. Kai, Solar Energy Materials & Solar Cells, 90 (2006) 1156.

[25] F. Li, X. Wang, C. Shao, R. Tan, Y. Liu, Mater. Lett.,61 (2007) 1328.

[26] Y. Yang, Q. Zhu, A. Jin, W. Chen, Solid State Ionics, 179 (2008) 1250.

[27] M.Kovendhan, D.Paul Joseph, P.Manimuthu, A.Sendilkumar, et al.,Current Applied Physics, 15 (2015) 622-631.

[28] V. Modafferi, G. Panzera, A. Donato, P.L. Antonucci, C. Cannilla, N. Donato, D. Spadaro, G. Neri, Sensors Actuators B, 163 (2012) 61-68.

[29] Ashvani Kumar, Preetam Singh, Nilesh Kulkarni, Davinder Kaur, Thin Solid Films, 516 (2008) 912 – 918.

[30] E. Gilles, E. Boesman, Phys. Status Solidi., 14(1966) 337-347.

[31] Yaoming Sun, Xiudi Xiao, Gang Xu, Guoping Dong, et al Scientific Reports, 3 (2013) 2756-2765.

[32] X.C. Song, E. Yang, G. Liu, Y. Zhang, Z.S. Liu, H.F. Chen, Y. Wang, J. Nanopart. Res.,12 (2010) 2813-2819.

[33] A.S. Reddy, N.M. Figueiredo, H.C. Cho, K.S. Lee, A. Cavaleiro, Mater. Chem. Phys., 133 (2012) 1024-1028.

[34] J.M. O-Rueda de Leon, D.R. Acosta, U. Pal, L. Castaneda, Electrochim. Acta, 56 (2011), 2599-2605.

[35] P. Scherrer, Bestimmung der Grösse und der inneren Struktur von Kolloidteilchen mittels, Rontgenstrahlen, Nachr. Ges. Wiss. Gottingen, 26 (1918) 98-100.

[36] M. Balaji, J. Chandrasekaran, M. Raja, Mater. Sci. Semicond. Process., 43 (2016) 104-113.

[37] V. Madhavi, P.J. Kumar, P. Kondaiah, O.M. Hussain, S. Uthanna, Ionics, (2014) DOI:10.1007/s11581-014-1073-8.

[38] K.J. Lethy, D. Beena, V.P.M. Pillai, V. Ganesan, J. Appl. Phys., 104 (2008) 033515(1-12).

[39] Li-Jian meng, Runi A. Silva, Hain-Ning Cui, Vasco Teixeira, M.P.dos santos, Zheng Xu, Thin solid Films, 515 (2006) 195-200.

[40] Ying Wang, Guozhong Cao, Electrochim. Acta, 51 (2006) 4865-4872.

[41] S. Senapati, S. Panda, Thin Solid Films, 599 (2016) 42–48.

[42] M. Balaji, J. Chandrasekaran, M. Raja, Mater. Sci. Semicond. Process., 43 (2016) 104-113.

[43] B.S. Acharcharya, B.B. Nayak, Microstructural studies of nanocrystalline thin films of V2O5-MoO3 using X-ray diffraction, optical absorption and laser micro Raman spectroscopy, Indian J. Pure Appl. Phys. 46 (Dec. 2008) 866e875.

[44] Chen W, Mai L, Qi V & Dai Yins, Phys & Chem Solids, 67(2006)896.

[45] V.S. Reddy Channu, Rudolf Holze, B. Rambabu, Rajamohan R. Kalluru, Quinton L. Williams, Chen Wen, Reduction of V4þ from V5þ using polymer as a surfactant for electrochemical applications Int. J. Electrochem. Sci. 5 (2010) 605e614

[46] Haro-Poniatowski E, Jouanne M, Morhange J F , Julien C, Diamant R, Fernadder-Guast M, Furntes GA, & Alonso J C, Aaal surface S, 127-129 (1998) 674.